Journal of the Korean Physical Society, Vol. 70, No. 5, March 2017, pp. 480∼488

Investigation of the Full Spectrum Phonon Lifetime in Thin Silicon Films from the Bulk Spectral Phonon Mean-Free-Path Distribution by Using Kinetic Theory

Jae Sik Jin*

Department of Mechanical Design, Chosun College of Science & Technology, Gwangju 61453, Korea

(Received 7 December 2016)

Phonon dynamics in nanostructures is critically important to thermoelectric and optoelectronic devices because it determines the transport and other crucial properties. However, accurately evaluating the phonon lifetimes is extremely difficult. This study reports on the development of a new semi-empirical method to estimate the full-spectrum phonon lifetimes in thin silicon films at room temperature based on the experimental data on the phonon mean-free-path spectrum in bulk silicon and a phenomenological consideration of phonon transport in thin films. The bulk of this work describes the theory and the validation; then, we discuss the trend of the phonon lifetimes in thin silicon films when their thicknesses decrease.

PACS numbers: 65.40.-b
Keywords: Phonon lifetime, Silicon thin film, Kinetic theory
DOI: 10.3938/jkps.70.480

I. INTRODUCTION

Phonon dynamics has been widely investigated both theoretically and experimentally due to its enormous importance to thermoelectric and optoelectronic devices [1–4]. When thermally induced phonons travel in a semiconductor or insulating nanostructure, all different phonon modes necessarily undergo continual scatterings among the phonons at various time intervals (*i.e.*, phonon lifetime, τ). In an analysis of phonon transport in both the bulk and nanostructures, complications arise from the estimate of τ because considerable detail is required for phonon scattering mechanisms such as phonon-phonon scattering, surface boundary scattering, impurity scattering, and so on; this is true even for simple crystalline semiconductors [5,6]. In an effort to estimate τ, notable works have been implemented theoretically by Klemens [7], Callaway [8], Holland [9], and Slack [10] based on low-frequency limits and considering several scattering mechanisms such as anharmonicity, defects, and dislocations. Because they used several fitting parameters in each model, these approaches have substantial limitations.

As a computational technique, the atomistic Green's functions [11] and molecular dynamics [12–14] were widely applied to calculate the thermal properties, but they gave limited insight onto the phonon properties. Recently, due to advances in both computer power and computational methods, first-principles anharmonic lattice dynamics calculations [15–20] have been done to calculate the phonon transport properties without any adjustable parameters. Phonon eigenvectors can be also used with a normal mode analysis to include the full anharmonicity of the interatomic potential [21].

While the first-principle approach is useful for understanding phonon transport physics, it has substantial limitations in addition to its high computational cost and complexity [22]: disagreement is still observed between first-principles calculations done by different researcher groups [6, 23]. A possible explanation for the observed differences is the effects of exchange-correlation and pseudopotential types on the density functional theory [22], the effect of macroscopic damping for low-energy phonons [23], and the dependency of anharmonicity on cutoff distances [18,24] which is important for determining the spectral anharmonic relaxation times [25] and, therefore, influences the multiple scatterings [26] used in their simulations, and leads to inaccuracies in the Gruneisen parameters [18,19].

Regarding the estimate of τ, one more thing needs to be pointed out: theoretical and computational methods mainly provide only the bulk τ [13,14,24,26–31] and shed no light on the phonon lifetimes (τ_{film}) in thin materials. Due to this lack of knowledge about τ_{film}, one should make a rough estimate of the thickness dependence of the conductivity; consequently, one should attempt to simulate the phonon transport in a material with a phenomenological scattering rate. Especially, the boundary

*E-mail: jinjs@cst.ac.kr

scattering relaxation time is considered to be the average time between two surface boundaries in the absence of intrinsic scattering, as employed by many authors [8,9, 30,32–40].

As for the measurement techniques, experimental studies of phonon lifetimes are more limited. Various experimental techniques, such as ultrasonic attenuation and velocity measurements [41], inelastic X-Ray scattering [42], picosecond acoustic measurements [43], pump-probe experiment using high-speed asynchronous optical sampling methods [5, 44–46], femtosecond electron diffraction [47], light scattering [48], femtosecond laser pump-probe techniques [49], and others, have been used to measure the phonon lifetimes in the bulk [41,43] and thin film [5,44–47,49] Si materials. Inelastic neutron scattering has also been applied to probe the lifetime of the optical phonon mode in single-walled carbon nanotubes [50]. Similar optical techniques have been employed to measure the phonon lifetimes in other material platforms such as MgB_2 [42], uranium dioxide [51], $AgSbTe_2$ [52], and the GaAs-AlAs superlattice [53]. Quietly recently, the minor carrier lifetimes in highly nitrogen-doped 4H-SiC epilayers were also measured [54].

Despite extensive experimental literature on phonon lifetimes in such various materials, their frequency ranges are always limited and less than several sub-THz because investigations at higher frequencies are strongly restricted by the driving and the detection methods [45]. At the same time, measured phonon lifetimes are only for coherent phonons, which is different from spontaneously thermal-induced phonons [55–57]. Maznev *et al.* [49] measured the spectral average phonon lifetimes of the acoustic longitudinal mode at 270 GHz in Si at room temperature. However, for Si at room temperature, the thermal transport is mostly conducted by phonon modes with frequencies above 1 THz [6,14,18,29,58].

Based on the above discussion, we concluded that there has no study of spectral phonon lifetimes in Si films over the whole range of the Brillouin zone (BZ) has been done at room temperature. The frequency dependence of the phonon lifetime in a Si film is one of the key properties associated with both thermal transport and ultrafast processes [59]. Especially, for transient heat conduction, the thermal decay rates are substantially different, depending on whether the boundaries are thermalizing or not [60]. Such studies require information on the spectral phonon lifetimes in Si films, for which few experimental data have been available until now.

In this work, we provide a new semi-empirical method to estimate the full-spectrum phonon lifetimes in thin-film Si at room temperature. To remove all assumptions used in the prior computational method, we find a clever way to employ experimental information on bulk properties such as the bulk mean free path (MFP) spectrum [61, 62] and the bulk thermal conductivity [24] because these bulk values already contain all intrinsic phonon scattering mechanisms. In this work, starting from this idea, we develop a new semi-empirical method for estimating the full-spectrum phonon lifetimes in Si films at room temperature based on the experimental data on the phonon MFP accumulation function (MFPAF) of bulk Si at room temperature [63] and the phenomenological consideration of phonon transport in thin films. We employed kinetic theory (KT) [64] to extract the spectral effective phonon MFP, which was determined by along the diffuse thermal transport part of the phonon spectrum; then, we discussed what happen to the phonon lifetimes as the film's thickness was decreased.

II. SEMI-EMPIRICAL METHOD

The semi-empirical framework of this work will be discussed. Considering τ is usually defined in terms of the MFP (Λ), $\Lambda = \tau \cdot v_g$ with the phonon group velocity (v_g), in principle, we can estimate directly from the MFP (*i.e.*, $\tau = \Lambda/v_g$). Thus, reliable quantitative results for the MFP spectrum are very much required for estimating τ. Recently, mean free path spectroscopy emerged as a useful technique for probing directly the thermal accumulation as a function of a wide range of MFP spectra by changing the size of the heat source in the experiment [58,63,65]. In such techniques, phonons with value of the MFP larger than a characteristic length are assumed to have ballistic transport and not to have any contribution to heat conduction. This simple assumption is reported to be not valid when the effects due to an anisotropy of the heat conduction caused by the nonequilibrium phonons, the effects of interfaces, and the effects of the dependency of the measured data on the phase of the induced temperature oscillations are not be negligibly small [23,66]. However, experimentally, an additional ballistic thermal resistance has been well demonstrated to originate from phonons with MFPs larger than a thermal length [39,67].

The main benefit of using data on the MFPAF [63] is that all the information on diffuse-phonon transport in the *net* direction of heat conduction can be employed in this study. For example, the amount of differential thermal conductivity (ΔK) is determined only by diffusive-transport part of the phonon spectrum (*i.e.*, their MFPs are less than a thermal length), and that part would be in the *net* direction of the heat conduction that is associated with an average over innumerable phonons originating from thermally excited atoms at one boundary and propagating in all directions, each with its own free path (see Fig. 1 for more detail). Yang and Dames [61] used the differential thermal conductivity to study the phonon transport along a Si thin film by using the Fuchs-Sondheimer equation and along a nanowire by using Matthiessen's rule to calculate the effective value of the MFP. Consequently, to gain a complete picture of the phonon dynamics from the MFPAF data [63], we have to do two tasks: determine the amount of ΔK corresponding to each phonon MFP and the frequency-dependent

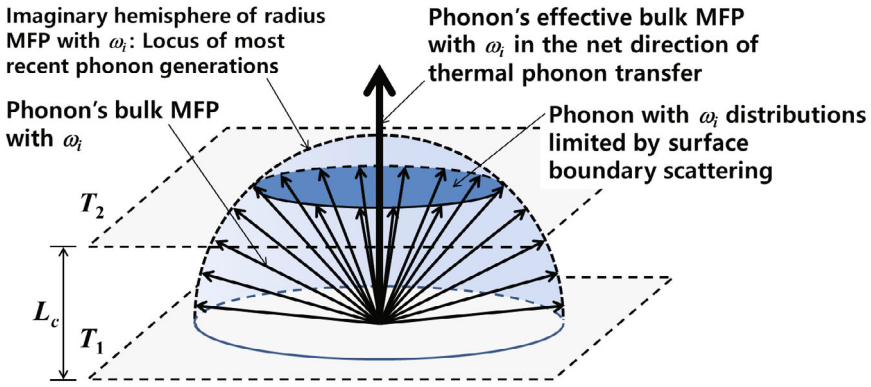

Fig. 1. (Color online) Schematic to explain the concept of the phonon's effective bulk mean free path at a particular phonon frequency (ω_i) in the net direction of thermal phonon transfer when $T_2 > T_1$.

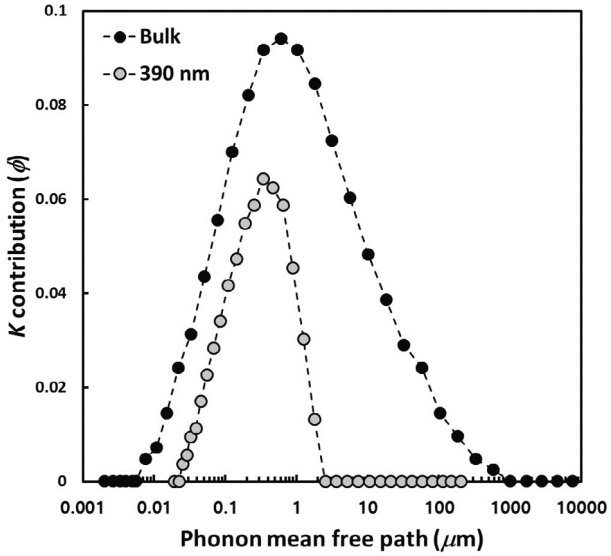

Fig. 2. Thermal conductivity (K) contribution as a function of the phonon's mean free path (MFP) showing how the K contribution (ϕ) varies with phonons having a specific MFP for the cases of bulk and 390 nm-thick Si at room temperature. The data were calculated from the experimentally measured phonon bulk MFP accumulation function at room temperature [63].

ΔK_ω.

1. Elicitation of the Amount of Differential Thermal Conductivity (ΔK)

To figure out how the phonon thermal conductivity (K) contribution (ϕ) varies with phonons having a specific MFP, we converted the accumulated data for the MFPAF into the differential amount, and we show the result in Fig. 2 for the cases of bulk and 390 nm-thick Si at room temperature. As Esfarjani *et al.* [18] and Minnich [63] discussed, thermal-induced phonons have an extremely broad spectrum with three orders of magnitude ($\sim$ 10 nm to $\sim$ 10 μm) of MFPs in Si at room temperature. Although phonons with MFPs larger than 1 μm contribute almost 50% to the overall thermal conductivity [14,18], Fig. 2 clearly reveals that we cannot neglect the contributions from other phonon modes. We also find that information from a wide range of MFP spectra can be taken from the bulk case, in stark contrast to the 390 nm case.

In the MFPAF data, reconstructed data for the bulk consist of 23 data points [63]. Based on the discrete MFPAF data, we can now find the differential thermal conductivity (ΔK_m) corresponding to the contribution of phonons with the m-th MFP (where m is the data number, *i.e*, $m = 1, 2, \ldots, 22, 23$) by using

$$\Delta K_m = K_{bulk} \left(\frac{d\phi}{d\Lambda} \right) \Delta\Lambda_m, \tag{1}$$

where K_{bulk} is the bulk thermal conductivity and $\Delta\Lambda_m$ is the differential MFP from Λ_{m-1} to Λ_{m+1}. Here, we emphasize that ΔK_m is the amount of thermal conductivity corresponding to the contribution of phonon modes with MFP comparable to a thermal characteristic length (L_c). In other words, ΔK_m can be used to calculate the effective MFPs determined by phonons under thermal equilibrium because phonons with a value of the MFP less than L_c will primarily contribute to heat conduction. Accordingly, the phonon distribution involving ΔK_m is close to an equilibrium state, and the contribution of phonons of a given frequency in a given branch to the total heat flux can be calculated just as a diffusive process.

2. Spectral Differential Thermal Conductivity (ΔK_ω)

Now, which phonon mode is involved in the spectral MFP is clear. Thus, we need to decompose the phonon-frequency-averaged MFPAF data into the contributions

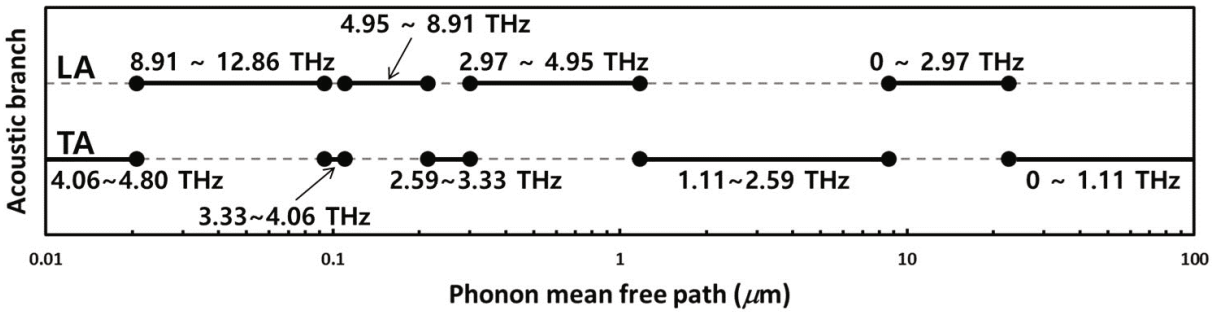

Fig. 3. Phonon frequency dependency of the mean free path distribution accounting for the phonon dispersion relation, showing which phonon frequency range corresponds to MFP distribution including polarization effects. The specific phonon frequency range was determined by considering three-phonon interaction processes, which are most likely to occur if their interactions (*i.e.*, energy exchanges) with other modes are constrained by energy and momentum conservation rules.

of different polarization branches. By so doing, separating the MFP spectrum into longitudinal acoustic (LA) and transverse acoustic (TA) phonon parts as a function of phonon frequency (ω) is very straightforward. From this information, we can determine the relation between the MFP and ω within the whole range of MFP spectra for the MFPAF. To do this, we need a reliable approach for predicting the spectral phonon MFP of solids qualitatively. Unfortunately, there is mostly unknown, even for a simple crystalline structure like Si, due to the dispersive nature of the phonon branches with the breadth of the phonon wavevector (k) spectrum.

In this study, we have resorted to calculating it by using the most commonly used approach. Han and Klemens [68] picked several types of three-phonon interaction processes that were most likely to occur if their interactions (*i.e.*, energy exchanges) with each other are constrained by energy and momentum conservation rules: LA + TA $\leftrightarrow$ LA; TA + TA $\leftrightarrow$ LA; TA + LA $\leftrightarrow$ LA; LA + TA $\leftrightarrow$ O; LA + LA $\leftrightarrow$ O; TA + LA $\leftrightarrow$ O; here O denotes the optical phonon mode. Through this approach, one can avoid unnecessary analytical complications in carrying out a more thorough analysis. This approach has been widely used for the simulation of thin-film conduction and has been demonstrated to recover the thermal conductivity of bulk Si [32,69,70]. It has also been employed by Cuffe *et al.* to calculate the total intrinsic phonon lifetime [46].

Actually, trying to compute innumerable scattering interactions during the transport of countless phonon modes in a solid is computationally very expensive. Therefore, the trick is to find a way to discretize the frequency spectrum by dividing it in a number of frequency ranges in a way that the nonlinear dispersion relation can be assumed to be a linear dispersion curve within the range. This approach is particularly convenient for our purposes because the corrected data from the MFPAF consist of 23 discrete data points and are not continuous. If more continuous data points are available, a more rigorous analysis should be developed (not shown here).

Each curve of the experimental dispersion relation in the [001] direction [71] is now discretized into 6 frequencies, in an equal-width frequency range of prescribed width ω ($\Delta\omega_{\mathrm{LA}} = 1.9788$ THz and $\Delta\omega_{\mathrm{TA}} = 0.7389$ THz). Of course, the accuracy of the solution is strongly influenced by the chosen $\Delta\omega$ range. The influence of the $\Delta\omega$ range has been tested, and the set of discretized width ω, yields results with an accuracy of about 3% for the computations of the thermal conductivity in bulk Si [32].

Using the expressions originally proposed by Han and Klemens [68], Narumanchi *et al.* provided the relaxation times for the interactions between different frequency ranges [72]. Their result is used here to figure out which phonon frequency range corresponds to the MFP distribution including polarization effects, and Fig. 3 shows the frequency dependency of the MFP distribution with the phonon dispersion relation. As expected, a low-frequency phonon mode has a long MFP. Here, we neglect the optical phonon contribution due to its negligibly small contribution to the thermal conductivity [38, 73]. Combining Eq. (1) and the relations for Λ_ω shown in Fig. 3, one can obtain the frequency-dependent ΔK_ω.

3. Effective MFPs Determined by using Diffusive-Transport Part of the Phonon Spectrum

An analytic theory based on the Boltzmann transport equation with the relaxation time approximation under the assumption of thermal equilibrium can be used to derive a classical kinetic theory [64], which is given by [1]

$$K_{bulk} = \frac{1}{3}\int C_\omega v_{g,\omega}\Lambda_{eff,EQ,\omega}d\omega, \tag{2}$$

where C_ω is the spectral specific heat and $v_{g,\omega}$, is the spectral phonon group velocity. That the spectral effective MFP ($\Lambda_{eff,EQ,\omega}$) is the effective value defined under local thermal equilibrium state is important to recognize. Based on Eq. (2), we can calculate $\Lambda_{eff,EQ,\omega}$,

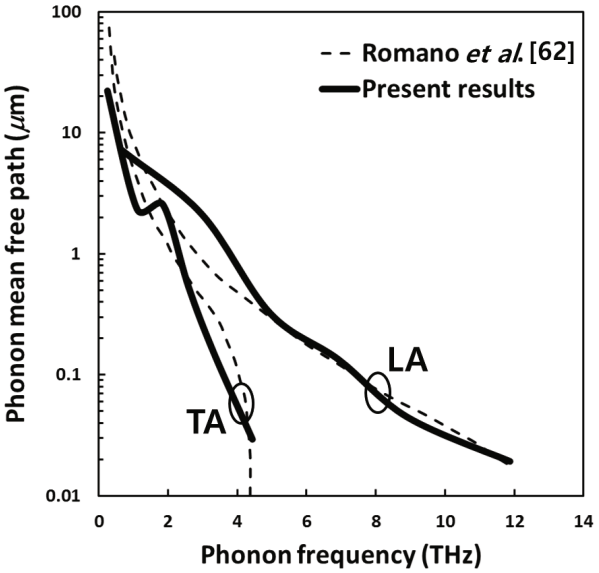

Fig. 4. Comparison of the obtained effective mean free path ($\Lambda_{eff,EQ,\omega}$) with that of Romano and Grossman [62] as a function of the phonon frequency. (LA: longitudinal acoustic phonons; TA: transverse acoustic phonons).

which is determined by using the diffusive-transport part of phonon spectrum, from the expression

$$\Lambda_{eff,EQ,\omega} = \frac{3\Delta K_\omega}{C_\omega v_{g,\omega}}. \quad (3)$$

Here, $v_{g,\omega}$ is calculated as $v_{g,\omega} = \partial\omega/\partial k$ from the experimental dispersion relation in the [001] direction [71] by assuming the crystals are isotropic [63, 70] because theoretically the anisotropy in phonon transport is dominantly observed for ultra-thin Si films [36, 74]. An explicit formula for C_ω in any acoustic branch can be found in Ref. [32].

At first look, the approach of using KT does not seem too bright for an analytical treatment considering the complicated diffusive phonon transport including the frequency dependencies of $C_\omega, v_{g,\omega}$, and $\Lambda_{eff,EQ,\omega}$. However, progress can be made if we recognize that Eq. (3) is available only under a thermal equilibrium condition and that only $\Lambda_{eff,EQ,\omega}$, (not C_ω or $v_{g,\omega}$) is involved in the thermal equilibrium process. Consequently, if we can obtain a reliable $\Lambda_{eff,EQ,\omega}$ for thin films, the KT-based approach can be applied to phonon transport in nanostructures. Figure 4 shows $\Lambda_{eff,EQ,\omega}$ for each polarization as a function of the phonon frequency. When comparing our results to those of Romano and Grossman [62], a difference between them can be easily seen to exist in the LA and the TA overlapping frequency ranges (*i.e.*, less than around 5 THz). A possible explanation for this observed difference is that in Romano and Grossman's calculations, the phonon normal scattering process is not included. Additionally, in this range, we strongly believed that coupling exists between LA and TA, which is neglected in their simulations.

4. Full-Spectrum Phonon MFPs and Lifetimes in Si Thin Films

Our goal is to calculate the full-spectrum phonon lifetime in Si thin films. Recall that the measured thermal conductivity of the MFPAF would be a thermal amount in the *net* direction of heat conduction. Therefore, the reduction of $\Lambda_{eff,EQ,\omega}$ by scattering at the boundaries (that is, film spectral MFP, $\Lambda_{film,eff,EQ,\omega}$), which is the elastic scattering process, can be simply calculated as

$$\Lambda_{film,eff,EQ,\omega} = L_c \text{ when } \Lambda_{eff,EQ,\omega} > L_c \text{ and}$$
$$\Lambda_{film,eff,EQ,\omega} = \Lambda_{eff,EQ,\omega} \text{ when } \Lambda_{eff,EQ,\omega} \le L_c. \quad (4)$$

We employed some crude method. However, we believed that this is a quite reasonable approach due to the physical views behind $\Lambda_{eff,EQ,\omega}$ (see Fig. 1 for more detail). Here, we assume that no phonon confinement effects (such as wave confinement effects) exist, except the reduction of the MFP due to boundary scattering [61, 75]. At the boundaries, we also assume that purely diffuse scattering is dominant because boundary scattering in a nanostructure was recently revealed to be almost or completely diffuse at room temperature [63, 75–77]. The effects of phonon-point defects and phonon-isotope scatterings are ignored in this study because their effects are small compared to the effect of phonon-phonon scattering at room temperature [77, 78]. Finally, using Eq. (4), we can estimate the full-spectrum phonon lifetimes in both bulk and thin-film Si as $\tau_{bulk,\omega} = \Lambda_{eff,EQ,\omega}/v_{g,\omega}$ and $\tau_{film,\omega} = \Lambda_{film,eff,EQ,\omega}/v_{g,\omega}$, respectively.

5. Summary of the Method

The core steps to implement our method are summarized below.

(1) Calculating ΔK from MFPAF data, which includes all intrinsic phonon scattering mechanisms: Here, two points are noteworthy: (a) ΔK is determined mainly by the diffusive-transport part of the phonon spectrum (*i.e.*, their MFPs are less than a thermal length); (b) The measured MFPAF data will be in the *net* direction of heat conduction and be associated with an average over innumerable phonons.

(2) Determining the phonon frequency-dependent ΔK: in this study, energy and momentum conservation rules are employed to determine the phonon interactions (*i.e.*, energy exchanges) that are most likely to occur between the phonon modes.

(3) Calculating from kinetic theory the effective bulk phonon MFP ($\Lambda_{eff,EQ,\omega}$) associated with such phonons in thermal equilibrium.

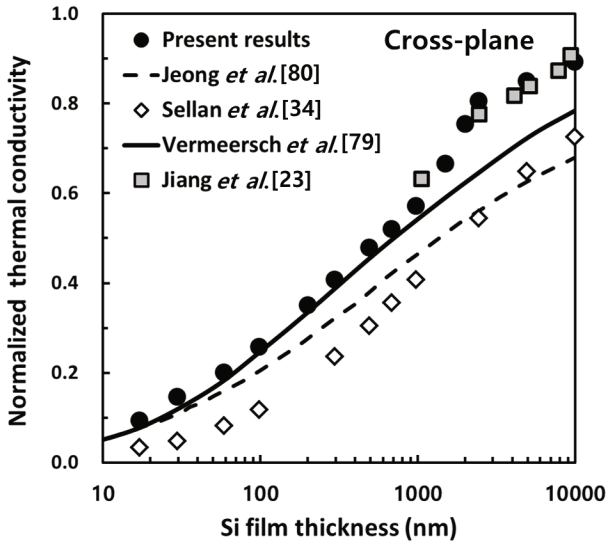

Fig. 5. Cross-plane thermal conductivity in thin films at room temperature compared to the data available in the literature. The present results (solid circles) lead to very excellent agreement with the most recent measurement data [23]. Bulk values used to normalize both calculated and experimental values were chosen from the literature; *i.e.*, 156, 157, and 143 W/mK were used for Jeong *et al.* [80], Vermeersch *et al.* [79], and Jiang *et al.* [23], respectively. For Sellan *et al.* [34], normalized values as presented by them were used. For the present results, the predicted bulk value of 147 W/mK was used. In addition, Jiang *et al.* [23] have defined $L_c = 3h_f/4$, where h_f is the film's thickness.

(4) Obtaining spectral phonon MFP in the thin film ($\Lambda_{film,eff,EQ,\omega}$) associated with phonon-boundary scattering by reducing $\Lambda_{eff,EQ,\omega}$, with a film thickness that is normal to the direction of heat conduction.

(5) Calculating the full-spectrum phonon lifetimes in Si thin film as $\tau_{film,\omega} = \Lambda_{eff,EQ,\omega}/v_{g,\omega}$,

III. VALIDATION OF THE SEMI-EMPIRICAL FRAMEWORK

To validate the applicability of the obtained effective MFPs, both $\Lambda_{eff,EQ,\omega}$ and $\Lambda_{film,eff,EQ,\omega}$, we used Eq. (2) combined with Eq. (4) to calculated the cross-plane thermal conductivity (K_{cross}). The result is shown in Fig. 5 and compared with very recently available K_{cross} measurement data [23] and first-principles calculations [79]. The simulation results of Jeong *et al.* [80] and Sellen *et al.* [34] are also plotted for comparison. From Fig. 5, one can see that comparison of our K_{cross} leads to very excellent agreement with the most recent data, even though we did not attempt to provide a rigorous method for separating the LA and the TA phonon contributions from the MFPAF spectrum data. This result is very desirable because, as done by Hua and Minnich [81] and Vermeersch and co-works [79], the cross-plane thermal conductivity of thin films can be calculated using substantially difficult and complicated methods.

Previously, for an estimate of the bulk phonon MFP from KT, incorporating only the spectral dependences of all relevant phonon properties might be sufficient to match the experimental data [82]. On the other hand, for an estimate of the phonon MFP in thin films, a suppression function is used to KT [81]. However, our results show the importance of considering the diffusive thermal transport part of the phonon spectrum when kinetic theory is used for phonon transport in nanostructures.

From a more fundamental point of view, however, basic questions go beyond the limitations of the current simulation techniques for computing the phonon lifetimes in thin films. The most vulnerable simplification used in our approach is the method to determine which phonon mode is involved in the MFP distribution. This leads to the application of energy and momentum conservation rules in determining the phonon interactions (*i.e.*, energy exchanges) that are most likely to occur with each of the other modes. Also, lack of experimental data on the full-spectral lifetimes of Si thin films precludes a judgment as to the reasonableness of our results. However, in our approach, we obtained successful results in the calculation of cross-plane thermal conductivity as a function of the film's thickness.

IV. FULL-SPECTRUM PHONON LIFETIMES IN SI THIN FILMS

To fully understand the spectral phonon lifetimes in Si thin films, we show the calculated phonon lifetimes for both bulk and thin-film Si in Fig. 6. Clearly, the values of τ for both the bulk and the thin film are obtained from Eq. (3) by assessing ΔK_m from Eq. (1). In Fig. 6, the thinnest film is as thin as 17.4 because Si thin films thicker than 17.4 nm have a bulk phonon density of states [33,74]. Actually, a confinement-induced modification of v_g due to a change in the acoustic phonon spectrum is observed in ultra-thin films [74], superlattices [83, 84], and nanowires [85]. Also represented in Fig. 6 are the phonon lifetimes of acoustic phonons, which were recently calculated including the phonon anharmonicity in bulk Si, predicted by Sellan *et al.* [34] and Esfarjani *et al.* [18]. The important thing is that Sellan *et al.* [34] calculated the LA and the TA combined phonon-phonon relaxation times by using anharmonic lattice dynamics simulations. Esfarjani *et al.* [18] employed first-principles calculations to develop a classical force field that could be used in the calculations of the anharmonic phonon lifetimes. They separated the normal and the umklapp components of the lifetimes by using $1/\tau = 1/\tau^U + 1/\tau^N$, where τ^U and τ^N are the lifetimes for the umklapp and the normal processes, respec-

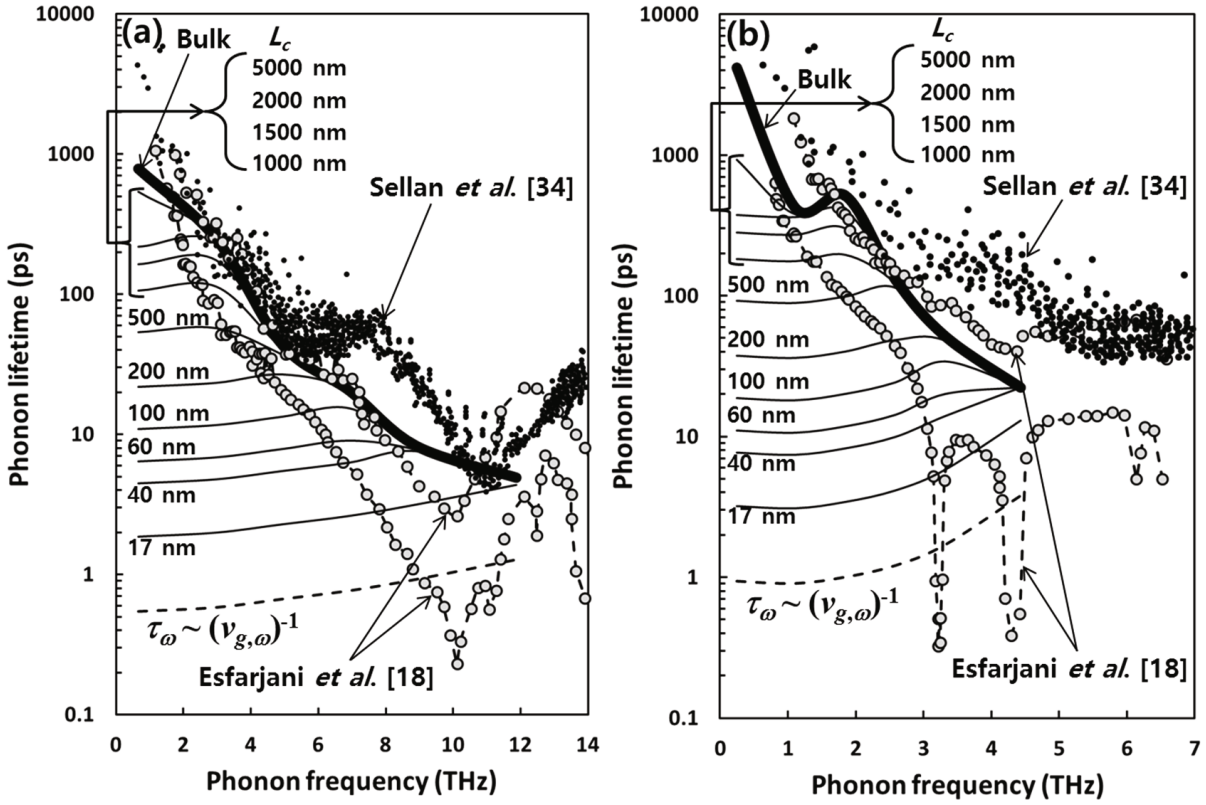

Fig. 6. Calculated phonon lifetimes in bulk and thin-film Si as functions of phonon frequency at room temperature: (a) phonon lifetimes for LA and (b) phonon lifetimes for TA. The simulations [18,34] are also included for comparison. Here, noting that Sellan *et al.* [34] calculated the LA and TA combined phonon-phonon lifetimes at room temperature is important. Also, because of the scatter in the calculated data of Esfarjani *et al.* [18] at 277 K, upper and lower values are plotted. Dotted lines show the relation of $\tau_\omega \sim (v_{g,\omega})^{-1}$.

tively. Therefore, the LA and the TA phonon lifetimes can be calculated by using $1/\tau_j = 1/\tau_j^U + 1/\tau_j^N$, where the subscript j is the LA or the TA mode. As can be seen in Fig. 6, the phonon lifetime calculations for bulk Si fall within the range of the simulation results, but they do exhibit some differences from those obtained by Esfarjani *et al.* [18], especially for high-frequency ranges. The thermal equilibrium state can be achieved by phonon interactions through two anharmonic processes (*i.e.*, the normal and the umklapp processes) [86]. For high-frequency phonons (roughly above 3 THz for both the LA and the TA modes), umklapp phonon scattering is the dominant transport mechanism [18]. Due to the dispersive nature of the phonon branches with the breadth of the phonon wavevector spectrum, we expect a great difficulty in evaluating the spectral U-process (*i.e.*, interphonon [87]) relaxation times qualitatively by using numerical simulations.

Now, we will discuss what happens to the phonon lifetimes as the film's thickness is decreased. As expected, the spectral τ distributions in thin films become more even than in the bulk case; that is, the lifetimes of low-frequency phonons are significantly reduced by boundary scattering while the lifetimes of high-frequency acoustic phonons are much less influenced. From these observations, the phonon lifetime will be inversely proportional to the phonon group velocity due to $\tau_\omega = \Lambda_\omega / v_{g,\omega}$, where Λ_ω approaches a constant value, the film's thickness, in nanostructures. Consequently, higher-frequency phonons become relatively long-lived energy carriers as the film's thickness is tuned to values below around a 40 nm thickness for both the LA and the TA modes. However, this trend also shows up for thicker films, such as films with thicknesses of several hundred nanometers, although it is limited more and more to the lower-frequency range as the film's thickness is increased. As a result, we conclude that when the dominant contribution to the thermal conductivity comes from the low-frequency phonons in Si, boundary scattering can be considered to be almost independent of the frequency. Therefore, the approximation $\tau_\omega \sim (v_{g,\omega})^{-1}$ gives successful analytical results for the cross-plane thermal conductivity of thin graphite flakes with thicknesses ranging from 24 nm to 714 nm along the c-axis of graphite at room temperature [88] because very long intrinsic phonon MFPs were observed in their experiment.

Phonon lifetimes are well known to be limited by intrinsic and extrinsic scatterings [5]. In this study, we

presented a separation of intrinsic and extrinsic effects in Si films, showing which one was the dominant contribution for various film thicknesses. Another point that has been made clear by our results is that for thicker films (*e.g.*, the 5000 nm- and 2000 nm-thick cases), the τ reduction is limited to frequency ranges below around 3 THz and 1.5 THz for the LA and the TA modes, respectively. For thinner films, τ is almost a constant over the whole range of frequencies, which indicates that in this region, phonon transport is strongly dominated by phonon-boundary scattering and intrinsic scattering only makes a marginal contribution. We note that sharp features such as the kink in τ_{LA} at around 2 THz cannot be explained here due to the averaging induced by the effective concept for obtaining $\Lambda_{eff,EQ,\omega}$.

V. CONCLUSION

We developed an approach for estimating reliable full-spectrum phonon lifetimes in Si thin films at room temperature. To overcome the limitations of the prior computational methods, we used the experimentally measured bulk phonon MFP accumulation function. We discussed what happened to the phonon lifetimes as the film's thickness was decreased, indicating a strong persistence of higher-frequency phonons in the nanostructures. The importance of considering the diffusive thermal transport part of the phonon spectrum when kinetic theory is used for phonon transport in nanostructures was also shown. Through this approach, a deep understanding of the phonon lifetime was attained. The approach presented here can be applied further to other materials like alloys and superlattices if MFPAF data are available.

REFERENCES

[1] G. Chen, *Nanoscale Energy Transport and Conversion* (Oxford University Press, New York, 2005).
[2] A. J. Minnich, J. Phys. Condens. Matter. **27**, 053202 (2015).
[3] W. Kim, J. Mater. Chem. C **3**, 10336 (2015).
[4] V. Chiloyan, L. Zeng, S. Huberman, A. A. Maznev, K. A. Nelson and G. Chen, Phys. Rev. B **93**, 155201 (2016).
[5] M. Grossmann, M. Klingele, P. Scheel, O. Ristow *et al.*, Phys. Rev. B **88**, 205202 (2013).
[6] A. A. Maznev, J. Appl. Phys. **113**, 113511 (2013).
[7] P. G. Klemens, *Solid State Physics*, edited by F. Seitz and D. Tumbull (Academic, New York, 1958), Vol. 7.
[8] J. Callaway, Phys. Rev. **113**, 1046 (1959).
[9] M. G. Holland, Phys. Rev. **132**, 2461 (1963).
[10] G. A. Slack, J. Phys. Chem. Solids **34**, 321 (1973).
[11] W. Zhang, T. S. Fisher and N. Mingo, Numer. Heat Tr. B-Fund. **51**, 333 (2007).
[12] A. J. C. Ladd, B. Moran and W. G. Hoover, Phys. Rev. B **34**, 5058 (1986).
[13] A. J. H. McGaughey and M. Kaviany, Phys. Rev. B **69**, 094303 (2004).
[14] A. S. Henry and G. Chen, J. Comput. Theor. Nanosci. **5**, 141 (2008).
[15] G. Deinzer, G. Birner and D. Strauch, Phys. Rev. B **67**, 144304 (2003).
[16] D. A. Broido, M. Malorny, G. Birner, Natalio Mingo and D. A. Stewart, Appl. Phys. Lett. **91**, 231922 (2007).
[17] J. Garg, N. Bonini, B. Kozinsky and N. Marzari, Phys. Rev. Lett. **106**, 045901 (2011).
[18] K. Esfarjani, G. Chen and H. T. Stokes, Phys. Rev. B **84**, 085204 (2011).
[19] A. Togo, L. Chaput and I. Tanaka, Phys. Rev. B **91**, 094306 (2015).
[20] A. Jain and A. J. H. McGaughey, Comput. Mater. Sci. **110**, 115 (2015).
[21] T. Feng, B. Qiu and X. Ruan, J. Appl. Phys. **117**, 195102 (2015).
[22] M. B. Bebek, C. M. Stanley, T. M. Gibbons and S. K. Estreicher, Sci. Rep. **6**, 32150 (2016).
[23] P. Jiang, L. Lindsay and Y. K. Koh, J. Appl. Phys. **119**, 245705 (2016).
[24] T. Shiga, D. Aketo, L. Feng and J. Shiomi, Appl. Phys. Lett. **108**, 201903 (2016).
[25] T. Shiga, T. Murakami, T. Hori, O. Delaire and J. Shiomi, Appl. Phys. Express **7**, 041801 (2014).
[26] H. Zhao and J. B. Freund, J. Appl. Phys. **104**, 033514 (2008).
[27] J. E. Turney, E. S. Landry, A. J. H. McGaughey and C. H. Amon, Phys. Rev. B **79**, 064301 (2009).
[28] J. V. Goicochea, M. Madrid and C. H. Amon, J. Heat Transfer **132**, 012401 (2010).
[29] A. Ward and D. A. Broido, Phys. Rev. B **81**, 085205 (2010).
[30] C. Ni and J. Y. Murthy, J. Heat Transfer **134**, 082401 (2012).
[31] T. Feng, B. Qiu and X. Ruan, Phys. Rev. B **92**, 235206 (2015).
[32] S. V. J. Narumanchi, J. Y. Murthy and C. H. Amon, J. Heat Transfer **126**, 946 (2004).
[33] J. E. Turney, A. J. H. McGaughey and C. H. Amon, J. Appl. Phys. **107**, 024317 (2010).
[34] D. P. Sellan, J. E. Turney, A. J. H. McGaughey and C. H. Amon, J. Appl. Phys. **108**, 113524 (2010).
[35] D. P. Sellan, E. S. Landry, J. E. Turney, A. J. H. McGaughey and C. H. Amon, Phys. Rev. B **81**, 214305 (2010).
[36] Z. Aksamija and I. Knezevic, Phys. Rev. B **82**, 045319 (2010).
[37] A. J. H. McGaughey and A. Jain, Appl. Phys. Lett. **100**, 061911 (2012).
[38] Z. Zhu, D. A. Romero, D. P. Sellan, A. Nabovati and C. H. Amon, J. Appl. Phys. **113**, 173511 (2013).
[39] T. S. English, L. M. Phinney, P. E. Hopkins and J. R. Serrano, J. Heat Transfer **135**, 091103 (2013).
[40] A. J. Minnich, Phys. Rev. B **91**, 085206 (2015).
[41] W. P. Mason and T. B. Bateman, J. Acoust. Soc. Am. **36**, 644 (1964).
[42] A. Shukla, M. Calandra, M. d'Astuto, M. Lazzeri *et al.*, Phys. Rev. Lett. **90**, 095506 (2003).
[43] B. C. Daly, K. Kang, Y. Wang and D. G. Cahill, Phys. Rev. B **80**, 174112 (2009).
[44] F. Hudert, A. Bruchhausen, D. Issenmann, O. Schecker

et al., Phys. Rev. B **79**, 201307 (2009).
[45] A. Bruchhausen, R. Gebs, F. Hudert, D. Issenmann *et al.*, Phys. Rev. Lett. **106**, 077401 (2011).
[46] J. Cuffe, O. Ristow, E. Chavez, A. Shchepetov *et al.*, Phys. Rev. Lett. **110**, 095503 (2013).
[47] M. Harb, W. Peng, G. Sciaini, C. T. Hebeisen *et al.*, Phys. Rev. B **79**, 094301 (2009).
[48] G. Rozas, M. F. P. Winter, B. Jusserand, A. Fainstein, B. Perrin, E. Semenova and A. Lemaitre, Phys. Rev. Lett. **102**, 015502 (2009).
[49] A.A. Maznev, F. Hofmann, J. Cuffe, J. K. Eliason and K. A. Nelson, Ultrasonics **56**, 116 (2015).
[50] D. Song, F. Wang, G. Dukovic, M. Zheng, E. D. Semke, L. E. Brus and T. F. Heinz, Phys. Rev. Lett. **100**, 225503 (2008).
[51] J. W. L. Pang, W. J. L. Buyers, A. Chernatynskiy, M. D. Lumsden, B. C. Larson and S. R. Phillpot, Phys. Rev. Lett. **110**, 157401 (2013).
[52] J. Ma, O. Delaire, A. F. May, C. E. Carlton, M. A. McGuire *et al.*, Nat. Nanotechnol. **8**, 445 (2013).
[53] A. A. Maznev, F. Hofmann, A. Jandl, K. Esfarjani, M. T. Bulsara, E. A. Fitzgerald, G. Chen and K. A. Nelson, Appl. Phys. Lett. **102**, 041901 (2013).
[54] T. Tawara, T. Miyazawa, M. Ryo, M. Miyazato *et al.*, J. Appl. Phys. **120**, 115101 (2016).
[55] J. Ravichandran, A. K. Yadav, R. Cheaito, P. B. Rossen *et al.*, Nat. Mater. **13**, 168 (2014).
[56] C-K. Sun, J-C. Liang and X-Y. Yu, Phys. Rev. Lett. **84**, 179 (2000).
[57] D. S. Kim, H. L. Smith, J. L. Niedziela, C. W. Li, D. L. Abernathy and B. Fultz, Phys. Rev. B **91**, 014307 (2015).
[58] J. A. Johnson, A. A. Maznev, J. Cuffe, J. K. Eliason *et al.*, Phys. Rev. Lett. **110**, 025901 (2013).
[59] F. Yang and C. Dames, Phys. Rev. B **91**, 165311 (2015).
[60] N. K. Ravichandran and A. J. Minnich, Phys. Rev. B **93**, 035314 (2016).
[61] F. Yang and C. Dames, Phys. Rev. B **87**, 035437 (2013).
[62] G. Romano and J. C. Grossman, J. Heat Transfer **137**, 071302 (2015).
[63] A. J. Minnich, Phys. Rev. Lett. **109**, 205901 (2012).
[64] F. Reif, *Fundamentals of statistical and thermal physics* (Waveland Press, Long Grove, 2009).
[65] A. J. Minnich, J. A. Johnson, A. J. Schmidt, K. Esfarjani, M. S. Dresselhaus, K. A. Nelson and G. Chen, Phys. Rev. Lett. **107**, 095901 (2011).
[66] Y. K. Koh, D. G. Cahill and B. Sun, Phys. Rev. B **90**, 205412 (2014).
[67] M. E. Siemens, Q. Li, R. Yang, K. A. Nelson, E. H. Anderson, M. M. Murnane and H. C. Kapteyn, Nat. Mater. **9**, 26 (2010).
[68] Y-J. Han and P. G. Klemens, Phys. Rev. B **48**, 6033 (1993).
[69] R. A. Escobar and C. H. Amon, J. Heat Transfer **130**, 092402 (2008).
[70] A. Mittal and S. Mazumder, J. Heat Transfer **132**, 052402 (2010).
[71] B. N. Brockhouse, Phys. Rev. Lett. **2**, 256 (1959).
[72] S. V. J. Narumanchi, J. Y. Murthy and C. H. Amon, J. Heat Transfer **127**, 713 (2005).
[73] A. J. Minnich, G. Chen, S. Mansoor and B. S. Yilbas, Phys. Rev. B **84**, 235207 (2011).
[74] H. Karamitaheri, N. Neophytou and H. Kosina, J. Appl. Phys. **113**, 204305 (2013).
[75] J. Cuffe, J. K. Eliason, A. A. Maznev, K. C. Collins *et al.*, Phys. Rev. B **91**, 245423 (2015).
[76] J. C. Duda, T. E. Beechem, J. L. Smoyer, P. M. Norris and P. E. Hopkins, J. Appl. Phys. **108**, 073515 (2010).
[77] A. Jain, Y-J. Yu and A. J. H. McGaughey, Phys. Rev. B **87**, 195301 (2013).
[78] R. K. Kremera, K. Grafa, M. Cardonaa, G. G. Devyatykh *et al.*, Solid State Commun. **131**, 499 (2004).
[79] B. Vermeersch, J. Carrete and N. Mingo, Appl. Phys. Lett. **108**, 193104 (2016).
[80] C. Jeong, S. Datta and M. Lundstrom, J. Appl. Phys. **111**, 093708 (2012).
[81] C. Hua and A. J. Minnich, J. Appl. Phys. **117**, 175306 (2015).
[82] J. Lee, J. Lim and P. Yang, Nano Lett. **15**, 3273 (2015).
[83] P. Hyldgaard and G. D. Mahan, Phys. Rev. B **56**, 10754 (1997).
[84] S-I. Tamura, Y. Tanaka and H. J. Maris, Phys. Rev. B **60**, 2627 (1999).
[85] C. Marchbanks and Z. Wu, J. Appl. Phys. **117**, 084305 (2015).
[86] R. Peierls, Ann. Phys. **3**, 1055 (1929).
[87] B. L. Huang, Z. Ni, A. Millward, A. J. H. McGaughey, C. Uher, M. Kaviany and O. Yaghi, Int. J. Heat Mass Transf. **50**, 405 (2007).
[88] Q. Fu, J. Yang, Y. Chen, D. Li and D. Xu, Appl. Phys. Lett. **106**, 031905 (2015).